ELSEVIER

Journal of Materials Processing Technology 71 (1997) 377–383

Journal of Materials Processing Technology

# Processing map for the hot working of near-α titanium alloy 685

V. Gopala Krishna [a,*], Y.V.R.K. Prasad [b], N.C. Birla [c], G. Sambasiva Rao [d]

[a] *RCMA (Materials), Kanchanbagh, Hyderabad 500 058, India*
[b] *Indian Institute of Science, Bangalore, India*
[c] *DMRL, Kanchanbagh, Hyderabad, India*
[d] *Regional Engineering College, Warangal, India*

Received 1 April 1996

**Abstract**

Using a dynamic materials model, processing and instability maps have been developed for near-α titanium alloy 685 in the temperature range 775–1025°C and strain-rate range of 0.001–10 $s^{-1}$ to optimise its hot workability. The alloy's β-transus temperature lies at about 1020°C. The material undergoes superplasticity with a peak efficiency of 80% at 975°C and 0.001 $s^{-1}$, which are the optimum parameters for α–β working. The occurrence of superplasticity is attributed to two-phase microduplex structure, higher strain-rate sensitivity, low flow stress and sigmoidal variation between log flow stress and log strain rate. The material also exhibits flow localisation due to adiabatic shear-band formation up to its β-transus temperature with strain rates greater than 0.02 $s^{-1}$ and thus cracking along these regions. © 1997 Published by Elsevier Science S.A.

*Keywords:* Near-α titanium alloy 685; Processing map; Hot working

## 1. Introduction

Near-α titanium alloy 685 possesses a complex constitution, having a nominal composition (wt.%) of Ti–6Al–5Zr–0.5Mo–0.25Si. The alloy has been developed mainly as forging stock, intended for critical aerospace components such as discs, shafts, etc. requiring moderate tensile strength, excellent creep resistance and superior fatigue strength up to 550°C. Newer demands of supersonic persistance and supercruise for improving survivability of increasingly expensive pilot and attack aircraft attach great importance in producing highly reliable forgings. Alloy 685 is essentially different from other α-base titanium alloys in that it is suitable for forging in the β-field [1]. However, excessive time at high temperatures, which result in grain coarsening, are to be strictly avoided. To achieve a match between engineering needs and the processing route, the traditional forger uses his skill and experience on a trial-and-error basis, resulting in excessive rejections. More recently, a 'right-first-time' philosophy has been introduced using science-based methodologies such as dynamic materials models to develop a processing map with the aim of tailoring the microstructure of the forging and to avoid defects such as flow instabilities on a repeatable basis in a manufacturing environment [2–4].

In dynamic materials models [5], metal processing is considered as a system in which the workpiece material is a dissipator of power. The power-dissipation characteristics of the workpiece depend upon the constitutive flow behaviour of the material, which follows a power-law equation:

$$\sigma = k \cdot \dot{\varepsilon}^m \tag{1}$$

where $\sigma$ is the flow stress, $\dot{\varepsilon}$ is the strain rate, $m$ is strain-rate sensitivity and $k$ is a constant. At any instant, the power dissipation occurs through a temperature rise ($G$ content) and a microstructural change ($J$ content). The factor that partitions the power is the strain-rate sensitivity $m$ of the flow stress $\sigma$. At a given temperature and strain, $J$ is given by [2]:

$$J = \sigma \cdot \dot{\varepsilon} \cdot m/(m+1) \tag{2}$$

where $\dot{\varepsilon}$ is the strain rate. The value of $J$ for a non-linear dissipator is normalised with that of a linear dissi-

* Corresponding author. Fax: +91 40 218827.


*PII* S0924-0136(97)00102-7

pator ($m=1$) to obtain a dimensionless parameter called the efficiency of power dissipation, given by:

$$\eta = \frac{J}{J_{max}} = \frac{2m}{m+1} \tag{3}$$

The variation of $\eta$ with temperature and strain rate constitutes a processing map, which exhibits various domains that may be correlated with specific microstructural mechanisms. The extremum principles of irreversible thermodynamics as applied to large plastic flow [6] are applicable to dynamic materials models. Kalyan Kumar [7] and Prasad [8] combined these principles with those of seperability of power dissipation and obtained a continuum criterion for obtaining flow instability during hot deformation, given by:

$$\zeta(\dot{\varepsilon}) = \frac{\delta \ln [m/(m+1)]}{\delta \ln \dot{\varepsilon}} + m < 0 \tag{4}$$

This method of modeling is effective despite several metallurgical processes occurring simultaneously during hot deformation and prior knowledge or evaluation of the atomistic mechanisms is not required. A method of understanding material behaviour which explicitly describes the dynamic metallurgical processes occurring during the hot deformation of alloy 685 has been presented in the present investigation.

## 2. Experimental

The chemical composition of alloy 685 material used in this investigation is given in Table 1. The initial material ($\beta$-forged), possesses acicular $\alpha$ (transformed $\beta$) and prior $\beta$-grain boundaries outlined by $\alpha$ that was

Table 1
Composition (wt.%) of alloy 685

| Element | Al | Zr | Si | Mo | H (ppm) | O (ppm) | Ti |
|---|---|---|---|---|---|---|---|
| Analysis | 6.12 | 5.1 | 0.24 | 0.52 | 35 | 1300 | Bal |

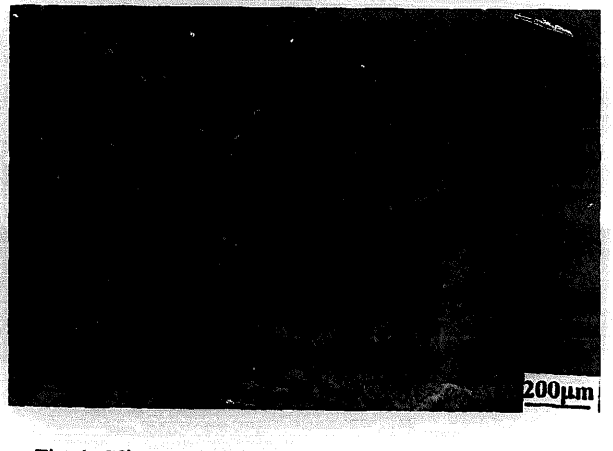


Fig. 1. Microstructure of the initial material: Alloy 685.

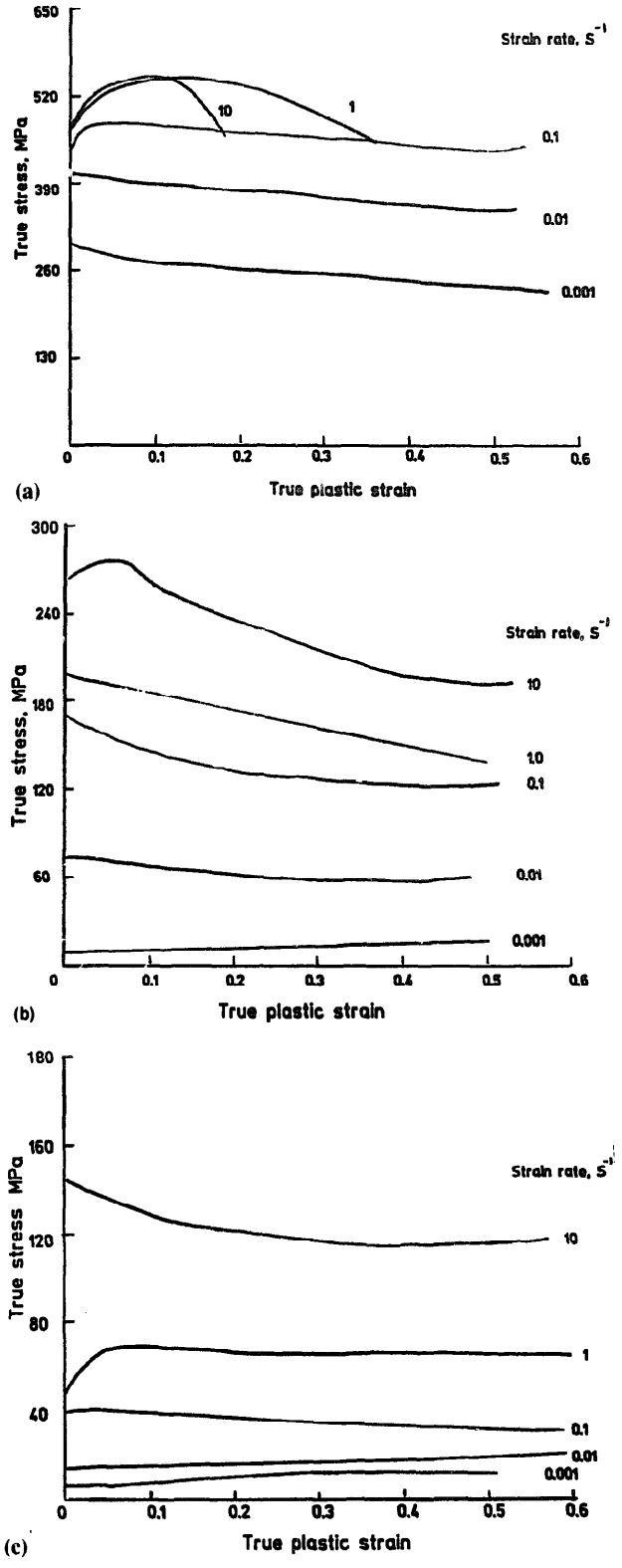


Fig. 2. A typical true stress–true strain curves of alloy 685 at: (a) 775; (b) 975; and (c) 1025°C at various strain rates.

the first to transform in its microstructure (Fig. 1). Cylindrical specimens of size 8 mm ∅, 12 mm height were machined from the initial material. Concentric grooves of about 0.5 mm depth were engraved on both of the end faces of the specimen to facilitate the reten-

Table 2
Flow stress (MPa) data at various strain rates and temperatures (corrected for adiabatic temperature increase)

| Strain | Strain rate ($s^{-1}$) | Temperature (°C) | | | | | |
|---|---|---|---|---|---|---|---|
| | | 775 | 825 | 875 | 925 | 975 | 1025 |
| 0.1 | 0.001 | 273.4 | 166.8 | 125.7 | 90.1 | 11.1 | 8.5 |
| | 0.01 | 391.4 | 304.4 | 203.9 | 122.8 | 68.8 | 15.8 |
| | 0.1 | 550.1 | 437.0 | 323.7 | 255.7 | 146.6 | 40.7 |
| | 1.0 | 674.0 | 554.0 | 434.0 | 314.0 | 191.0 | 71.0 |
| | 10 | 599.0 | 572.0 | 545.0 | 455.0 | 281.0 | 133.0 |
| 0.2 | 0.001 | 265.5 | 163.5 | 124.8 | 85.1 | 12.6 | 10.9 |
| | 0.01 | 383.6 | 302.8 | 193.3 | 124.1 | 62.8 | 16.5 |
| | 0.1 | 551.3 | 421.1 | 306.8 | 240.1 | 133.5 | 38.3 |
| | 1.0 | 656.0 | 542.0 | 425.0 | 308.0 | 191.0 | 71.0 |
| | 10 | 548.0 | 527.0 | 497.0 | 425.0 | 272.0 | 123.0 |
| 0.3 | 0.001 | 256.7 | 164.6 | 127.1 | 86.1 | 14.1 | 12.5 |
| | 0.01 | 374.5 | 293.3 | 182.9 | 122.7 | 59.5 | 17.6 |
| | 0.1 | 528.1 | 417.5 | 302.9 | 231.9 | 127.4 | 35.8 |
| | 1.0 | 599.0 | 497.0 | 389.0 | 284.0 | 176.0 | 67.0 |
| | 10 | 530.0 | 491.0 | 434.0 | 314.0 | 215.0 | 117.0 |
| 0.4 | 0.001 | 246.3 | 161.1 | 131.2 | 86.6 | 15.3 | 11.9 |
| | 0.01 | 358.1 | 278.3 | 181.8 | 121.1 | 57.5 | 18.4 |
| | 0.1 | 518.1 | 405.3 | 294.2 | 226.9 | 123.5 | 34.2 |
| | 1.0 | 548.0 | 452.0 | 359.0 | 263.0 | 164.0 | 67.0 |
| | 10 | 545.0 | 461.0 | 374.0 | 290.0 | 203.0 | 115.0 |
| 0.5 | 0.001 | 235.8 | 155.7 | 141.4 | 83.9 | 16.3 | 11.1 |
| | 0.01 | 352.9 | 275.0 | 202.4 | 212.7 | 62.1 | 19.4 |
| | 0.1 | 490.0 | 411.1 | 302.2 | 231.4 | 123.2 | 32.5 |
| | 1.0 | 545.0 | 452.0 | 356.0 | 263.0 | 164.0 | 66.0 |
| | 10 | 380.0 | 350.0 | 344.0 | 308.0 | 212.0 | 116.0 |

tion of lubricant. A chamfer of 1 mm at 45° was machined along the edges of the faces to avoid fold-over in the initial stages of compression. A 0.5 mm ∅ hole with a depth of 4 mm was also made at the mid height of the specimen for the insertion of a thermocouple.

Hot compression tests were carried out on a computer-controlled servo-hydraulic testing machine, which machine can be operated with an exponential decay of actuator speed to give constant true strain rate with strain. In deriving the exponential-decay equation for the stroke variation, the small elastic deflections of the machine and the grips were neglected. The accuracy of the temperature controller was within ±2°C and the adiabatic temperature increase during compression was measured using a thermocouple embedded in the specimen. Deformation was carried in the temperature range of 775–1025°C at strain rates of 0.001, 0.01, 0.1, 1 and 10 $s^{-1}$. In each case, the specimen was compressed to about half of its height (0.5 strain). Prior to hot compression testing, borosilicate glass powder (delta glaze) coating was applied to the specimens, to act not only as a lubricant but also as a protective coating against oxidation at the testing temperatures.

From the load–stroke data, true stress–true strain curves were evaluated using standard equations. The flow-stress data pertaining to different temperatures and strain rates were corrected for the adiabatic temperature increase. Using this data, power-dissipation maps were constructed for different strains by fitting log flow stress $v_s$ log strain-rate data at a constant temperature and strain rate using a cubic spline function, the strain-rate sensitivity $m$ being calculated as a function of strain rate. This was repeated at different temperatures. The efficiency of power dissipation through microstructural changes (Eq. (3)) was then calculated as a function of temperature and strain rate and plotted as a three-dimensional map and an iso-efficiency contour map. The data were also used to evaluate the instability parameter $\zeta(\dot{\varepsilon})$ (Eq. (4)) as a function of temperature and strain rate to obtain an instability map. After deformation, selected specimens were sectioned vertically at the centre (parallel to the compression axis) and prepared for metallographic examination using standard procedures. The specimens were etched with Kroll's reagent. Some selected specimens were also examined for microstructural features using a 300 KV Philips ET430T transmission electron microscope. The polishing reagent used was 6% sulphuric acid in methanol, the temperature of polishing being maintained at around −45°C.

## 3. Results

True stress–true strain curves, plotted as a function of strain rate at 775, 975 and 1025°C are shown in Fig. 2(a)–(c), respectively. The stress–strain curves pertaining to specimens deformed at or above 0.01 $s^{-1}$ exhibited flow softening. Corrected flow-stress data, obtained at different temperatures, strain rates and strains are given in Table 2.

Typical power-dissipation maps obtained at 0.2 and 0.4 strains are presented in Fig. 3(a) and (b), respectively. The maps at other strains are essentially similar. The maps exhibited a domain centred around 975°C and 0.001 $s^{-1}$. A map showing the contours of instability parameter $\zeta(\dot{\varepsilon})$ on a temperature–strain rate plane

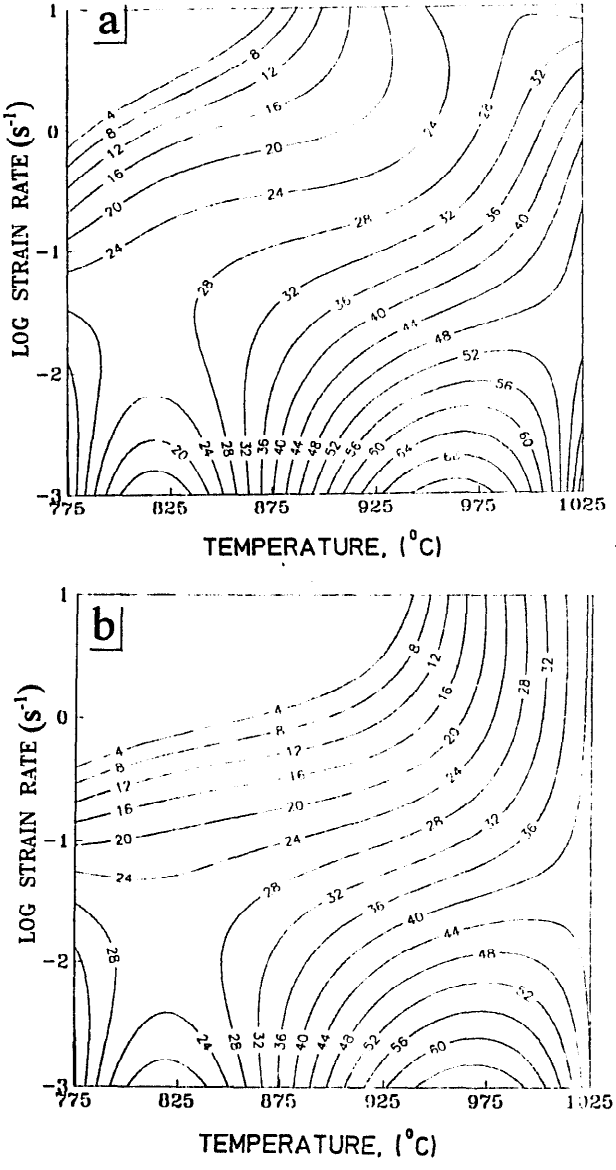


Fig. 3. Power dissipation maps for the alloy 685 at strains of: (a) 0.2; and (b) 0.4. The number against each contour indicates percentage efficiency.

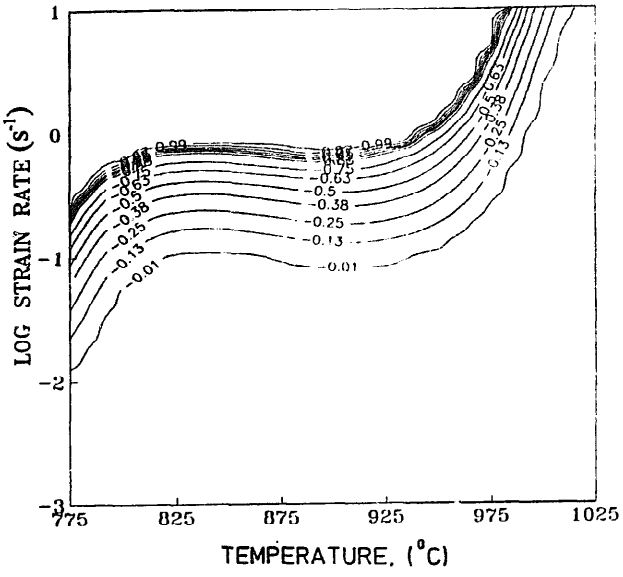


Fig. 4. Instability maps for alloy 685, showing contours on the temperature–strain-rate plane, for 0.4 strain.

for 0.4 strain is shown in Fig. 4. The instability region for the alloy under investigation lies almost up to its $\beta$ transus temperature (1020°C) for strain rates above 0.02 $s^{-1}$.

## 4. Discussion

The processing domain (corresponding to high efficiency), occurring at strain rates lower than 0.01 $s^{-1}$, shows a change in curvature of contours at about 1020°C, indicating the $\beta$-transus temperature of the alloy and conforming to literature values [1]. Microstructural examination of specimens deformed at 925, 975 and 1025°C and a strain rate of 0.001 $s^{-1}$ was conducted. Specimen deformed at 925°C exhibited a tendency of breaking up of acicular $\alpha$ (Fig. 5), present in the initial microstructure. The microstructure obtained for the specimen deformed at 975°C revealed sluggish coarsening of $\alpha$ laths, particularly at grain interiors and the formation of equi-axed $\alpha$ (Fig. 6). The sluggishness of the $\alpha$ phase can be attributed to slow kinetics of equilibration close to the $\beta$-transus temperature [9,10]. Transmission electron micrographs of the specimen deformed at 975°C and 0.001 $s^{-1}$ exhibited a mixture of sub-grains and lath $\alpha$ (Fig. 7). It has been shown that such micro-duplex structures favourably influence superplasticity at these temperatures in titanium alloys [11]. However, microstructural evidence for superplasticity is inconclusive, since transformation occurs during cooling and the resultant microstructure depends on the cooling rate. Further, signatures of the dynamic processes occurring during superplastic deformation are also not retained in the microstructure in view of the transformation during cooling.

One of the pre-requisites for obtaining superplasticity in titanium alloys is its two-phase structure [12] and the total elongation is strongly influenced by the ratio of two phases present at the deformation temperature concerned [13]. A 50:50 mixture of $\alpha$ and $\beta$ phases is generally considered optimum for superplasticity [14], since the mixture of these two phases can contribute to

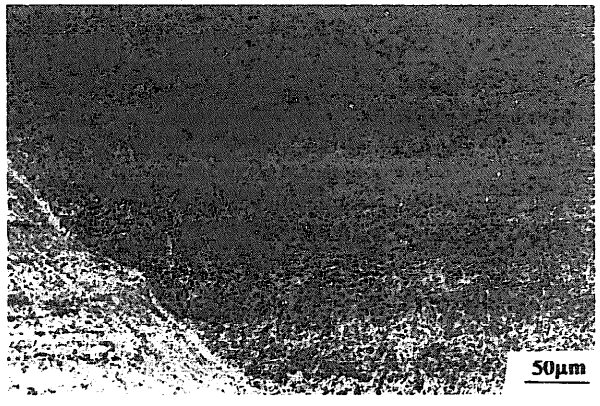


Fig. 5. Microstructure of a specimen deformed at 925°C and 0.001 $s^{-1}$ showing the tendency of the breaking-up of the acicular $\alpha$.


Fig. 6. Microstructure of a specimen deformed at 975°C and 0.001 $s^{-1}$, revealing sluggish coarsening of $\alpha$ laths, particularly at grain interiors.


Fig. 7. Transmission electron micrograph of a specimen deformed at 975°C and 0.001 $s^{-1}$, exhibiting a mixture of sub-grains and $\alpha$ laths.

Table 3
Values of strain-rate sensitivity ($m$) obtained at different testing temperatures and strains for a strain rate of 0.001 $s^{-1}$

| Testing temperature (°C) | Strain | | | | |
|---|---|---|---|---|---|
| | 0.1 | 0.2 | 0.3 | 0.4 | 0.5 |
| 775 | 0.16 | 0.16 | 0.16 | 0.16 | 0.17 |
| 825 | 0.26 | 0.26 | 0.25 | 0.24 | 0.24 |
| 875 | 0.20 | 0.19 | 0.16 | 0.14 | 0.15 |
| 925 | 0.13 | 0.14 | 0.13 | 0.12 | 0.15 |
| 975 | 0.80 | 0.70 | 0.62 | 0.58 | 0.58 |
| 1025 | 0.27 | 0.18 | 0.15 | 0.18 | 0.25 |

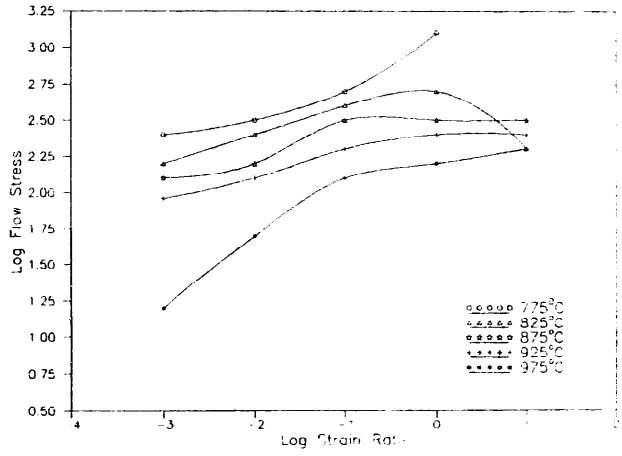


Fig. 8. Plot of log flow stress vs. log strain rate for different testing temperatures at 0.4 strain.

grain boundary sliding and accommodation [15]. The superplastic elongations at these volume fractions vary from 500 to 900%. Although the amounts of the volume fractions of $\alpha$ and $\beta$ phases present in the alloy 685 are not available in the literature, another near-$\alpha$ alloy with $\beta$-transus temperature close to this alloy contains 50:50 of $\alpha$ and $\beta$ phases at 975°C [16].

Strain-rate sensitivity $m$ usually characterises the superplasticity [17], these values for titanium alloys rang-


Fig. 9. Microstructure of a specimen deformed at 875°C and 10 $s^{-1}$ exhibiting a crack path oriented at about 45° to the compression axis, along with an adiabatic shear-band zone.

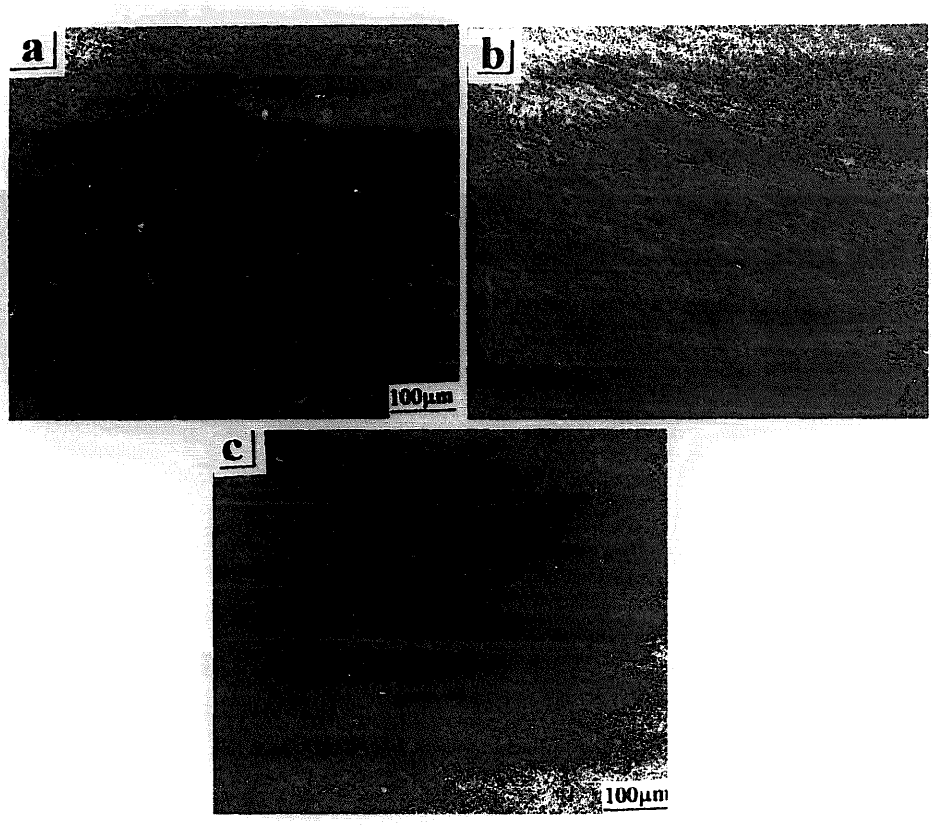


Fig. 10. Microstructure of specimens deformed at 875°C and different strain rates: (a) 1.0 $s^{-1}$, crack and adiabatic shear-band zone with very fine grains; (b) 0.1 $s^{-1}$, presence of an adiabatic shear-band zone; and (c) 0.01 $s^{-1}$, absence of an adiabatic shear-band zone.

ing from 0.4 to 0.9 [18]. From the flow stress data of Table 2, the slopes $m$ of the stress–strain curves have been calculated at all testing temperatures for different strains at a strain rate of 0.001 $s^{-1}$, using a power law (Eq. (1)). Results are given in Table 3. The values so obtained at 975°C fall within the superplastic range. It is also evident from the results in Table 3 that the strain-rate sensitivity $m$ decreases with strain during constant strain-rate deformation. This decrease is consistent with hardening and can therefore be attributed primarily to the growth of recrystallised grains [19].

Another characteristic feature, which enables one to conclude that the deformation is superplastic, is a typical sigmoidal relationship between log flow stress and log strain rate at that deformation temperature [20]. A plot of log flow stress versus log strain rate for testing temperatures below the $\beta$-transus of alloy 685 at 0.4 strain is shown in Fig. 8. It is evident that the slope increases with increasing temperature in the case of specimen deformed at 975°C, thus displaying sigmoidal relation.

On the basis of the above observations, i.e. two-phase micro-duplex structure, higher strain-rate sensitivity, sigmoidal relationship between log flow stress and log strain rate and low flow stresses (Table 2), the domain formed at 975°C and a strain rate of 0.001 $s^{-1}$ may be attributed to superplasticity.

## 5. Manifestation of instabilities

The material exhibits flow instabilities at strain rates greater than 0.025 $s^{-1}$ and temperatures up to its $\beta$-transus temperature, i.e. 1020°C (Fig. 4). Microstructural examination of the specimen deformed at 875°C and a strain rate of 10 $s^{-1}$ exhibited a crack path, oriented at about 45° to the compression axis, along with an adiabatic shearband zone (Fig. 9). The intense shear localisation in the band region has resulted in the formation of a very fine grain transformed microstructure along the crack length. The intensity of shear localisation, thus cracking tendency, has reduced as the strain rate is decreased and is absent in the sample deformed at 875°C and 0.01 $s^{-1}$. Fig. 10(a)–(c) show the phenomenon clearly.

## 6. Conclusions

Near-$\alpha$ titanium alloy 685 exhibits the following hot deformation characteristics.

(1) The alloy undergoes superplasticity in the temperature range 900–1020°C at strain rates of less than 0.02 $s^{-1}$. The micro-duplex structure in this region possesses partially recrystallised $\alpha$ and plate-like $\alpha$ in a transformed $\beta$-matrix.

(2) Alloy 685 possesses poor workability up to its $\beta$-transus temperature at conventional strain rates. However, the optimum conditions for $\alpha$–$\beta$ working lie at 975°C and strain rates lower than 0.02 $s^{-1}$.

(3) At temperatures of up to 1020°C and strain rates greater than 0.02 $s^{-1}$, the material exhibits flow instability, manifested as adiabatic shear-bands. These conditions must be avoided in processing the alloy.

## Acknowledgements

The first author expresses his gratitude to RCMA (Materials), Hyderabad, India, for giving permission for the publication of this work; M/s MIDHANI, Hyderabad, India for the supply of material; and IISc, Bangalore, India, for the provision of testing facilities for the carrying out of the present investigation.

## References

[1] Brochure of Imperial Metal Industries, UK, on Titanium alloy 685.
[2] Y.V.R.K. Prasad, H.L. Gegel, S.M. Doraivelu, J.C. Malas, J.T. Morgan, K.A. Lark, D.R. Barker, Metall. Trans. A15 (1984) 1883–1892.
[3] H.L. Gegel, J. Malas, S.M. Doraivelu, V.A. Shende, Forming and Forging, ASM Metals Handbook, vol. 14, 1988, pp. 417–438.
[4] J.M. Alexander, in: J.C. Lenard (Ed.), Modeling of Hot Deformation of Steels, Springer-Verlag, Berlin, 1984, pp. 101–114.
[5] Y.V.R.K. Prasad, J. Technol. 28 (1990) 435–451.
[6] H. Ziegler, in: I.N. Sneddon, R. Hill (Eds.), Progress in Solid Mechanics vol. 4, North Holland, Amsterdam, 1963, pp. 93–193.
[7] A.K.S. Kalyan Kumar, Criteria for predicting metallurgical instabilities in processing, MSc (Eng) Thesis, Indian Institute of Science, Bangalor, India, 1987.
[8] Y.V.R.K. Prasad, Ind. J. Technol. 28 (1990) 435.
[9] W.W. Cias, Continuous Cooling Transformation Kinetics of IMI685 and IMI 550 Titanium Alloys, Report No. Rp-27-72-08, Climax Molybdenum, Ann Arbor, MI, 1973.
[10] C.H. Hamilton, Superplasticity in Titanium Base Alloy: A Review, Proceedings MRS International Meeting on Advanced Materials, vol. 7, 1989, pp. 59–75.
[11] N. Ridley, Mater. Sci. Technol. 6 (1990) 1145–1156.
[12] P.J. Winkler, in: P. Lacombe, R. Tricot, G. Beranger (Eds.), Recent Advances in Superplasticity and Superplastic Forming of Titanium Alloys, Sixth World Conference on Titanium, France, Part III, 1988, pp. 1135–1150.
[13] C.H. Hamilton, in: Suphal P. Agarwal (Ed.), Superplasticity in Titanium Alloys, Proceedings of the Conference on Superplastic Forming, ASM, OH, 1985, pp. 13–22.
[14] F.H. Froes, W.T. Highberger, J. Met. 32 (1980) 57–64.
[15] R.C. Gifkins, Met. Trans. A7 (1976) 1225.
[16] P.A. Blenkinsop, High Temperature Titanium Alloys, Materials in Aerospace, vol. 1, The Royal Aeronautical Society, London, 1986, pp. 189–208.
[17] F.N. Lake, D.J. Moracz, Technical Report AFML-TR-71-112, TRW, Cleveland, OH, 1971.
[18] O.D. Sherby, R.D. Caligiuri, F.S. Kayali, R.A. White, in: J.J. Burke, R. Mahrabian (Eds.), Advances in Metal Processing, Plenum Press, New York, 1981, pp. 133–171.
[19] C.H. Hamilton, A.K. Ghosh, Characterisation of superplastic deformation properties of Ti-6Al-4V, in: H. Kimura, O. Izumi (Eds.), Proceedings of the Fourth International Conference on Ti, Titanium-80, vol. 2, 1980, pp. 1001–1014.
[20] O.D. Sherby, J. Wadsworth, Deformation Processing and Structure, ASM, Metals Park, OH, 1984.